EARTHQUAKE ENGINEERING AND STRUCTURAL DYNAMICS
Earthquake Engng. Struct. Dyn. **27**, 543–556 (1998)

NUMERICAL EFFICIENCY ASSESSMENT OF ENERGY DISSIPATORS FOR SEISMIC PROTECTION OF BUILDINGS

D. FOTI[1], L. BOZZO[2] AND F. LÓPEZ-ALMANSA[1,*]

[1] *Technical University of Catalonia, Department of Architecture Structures, Avda. Diagonal 649, 08028 Barcelona, Spain*
[2] *University of Girona, Department of Construction Engineering and Architecture, Avda. Lluís Santaló s/n, 17003 Girona, Spain*

SUMMARY

This paper presents a two-dimensional numerical study on the nonlinear seismic response of buildings equipped with two types of energy dissipators: Constant Friction Slip Braces (CFSB) and Adding Damping and Stiffness (ADAS). Three types of reinforced concrete buildings with 3, 7 and 15 storeys, representatives of the short-medium- and long-period ranges, are considered. Dissipators are placed in steel diagonal braces in all the floors. The sliding threshold (or yielding) forces for each mechanism are selected using two different criteria: (i) they are taken as 50, 75 and 100 per cent of those generated by the equivalent static lateral forces recommended by the UBC-91 for a ductile moment resisting frame and (ii) they are constant in the whole building (this constant value is chosen equal to the maximum forces obtained with the previous criterion). The input consists of ten recorded earthquakes (normalized with respect to their Housner intensity) corresponding to medium and stiff local soil conditions. Average values on the ten registers are given for the maximum horizontal displacement, the base shear, the energy dissipated and the interstorey drift. The possibility of failure in some devices has been numerically simulated to assess the robustness of the system. The obtained results show that both devices are useful to reduce the response compared to the bare frame and that CFSB is more efficient than ADAS; for 7- and 15-storey frames the lateral displacement with CFSB is even smaller than the one for the braced frame (rigid connections instead of dissipators). The conclusions are expected to provide simple design guidelines. © 1998 John Wiley & Sons, Ltd.

KEY WORDS: ADAS; CFSB; energy dissipators; preliminary design; parametric assessment; passive control

1. INTRODUCTION

Much of the existing research in energy dissipation systems focuses on experimental testing of particular devices[1,2] and in a lower extent there are numerical analysis of buildings equipped with dissipators.[3–5] Several papers presenting design rules have been published[6–9] but there is not a comprehensive study on the seismic efficiency of such systems. This paper presents a numerical nonlinear parametric assessment on the seismic response of buildings equipped with energy dissipation devices.

The study consists of assessing the 2-D seismic dynamic response of three reinforced concrete frames (with, respectively, 3, 7 and 15 storeys) equipped with energy dissipators. This research shows that such devices are efficient to reduce earthquake induced forces and at the same time maintaining interstorey drifts between reasonable bounds provided their number is enough and they are properly designed. In this paper the

* Correspondence to: F. López-Almansa, Departamento de Estructuras en la Arquitectura, ETSAB (UPC), Avda. Diagonal, 649, 08028 Barcelona, Spain. E-mail: lopez@ea.upc.es

Contract/grant sponsor: DGICYT; Contract/grant number: PB92-075
Contract/grant sponsor: European Commission; Contract/grant number: ERBCHBICT 941821

CCC 0098–8847/98/060543–14$17·50

Received 25 June 1997
Revised 1 August 1997

parameters of the dissipators are not necessarily constant along the height of the building. Previous research is often based on assuming that all the dissipators are alike; there are studies about the optimal variation of the properties for viscous dampers, but it can be costly to construct those dampers if their sizes are non-uniform or too big.[10] Conversely, energy dissipation mechanisms based on plastification of metals such as Adding Damping and Stiffness (ADAS) or friction of plates Constant Friction Slip Braces (CFSB) are easy to manufacture and their yielding force can be easily altered changing the thickness and number of plates or modifying the prestressing force and friction coefficient, respectively. Consequently, both devices are considered in this paper.

Seismic response of buildings incorporating dissipators cannot be efficiently represented by general non-linear models because the structure remains in the elastic range and nonlinearities concentrate in the dissipators. Besides, these algorithms may not describe accurately their hysteretic behaviour. Therefore, specific models have to be considered. In this paper the SADSAP computer program[11] has been used; the behaviour of the concrete frame and of the braces is linear and the yielding of the dissipators is represented by equation (1).

One of the objectives of this paper is to join two separate design approaches: classical earthquake engineering design based on ductility and more recent energy dissipation design mainly based on equivalent damping. A design trend should be the integration between these two approaches. Dissipators based on friction and plastification of metals (that could be analyzed with classical ductility tools) have been selected.

This study belongs to a bigger research project[12] (funded by the European Commission) that involves experimental tests as well.

2. DESCRIPTION OF THE STUDY

This section describes the elements of the study. In the first, second and third subsections, the dissipators, the buildings and the ground motions are depicted, respectively.

2.1. Energy dissipation devices

In this study two types of dissipators are considered: ADAS and CFSB. The ADAS device dissipates energy through the plastification of metal plates[13] and CFSB does through friction[14]; both are representative of the frequency-dependent and frequency-independent behaviours, respectively. In Figure 1 there is a representation of typical connections and hysteresis loops for both devices.

A general expression to describe the hysteretic response of energy dissipation connections is

$$\begin{aligned} F &= kd, \quad |d| \leqslant d_y \\ F &= kd_y \left(\frac{d}{d_y}\right)^n, \quad |d| \geqslant d_y \end{aligned} \tag{1}$$

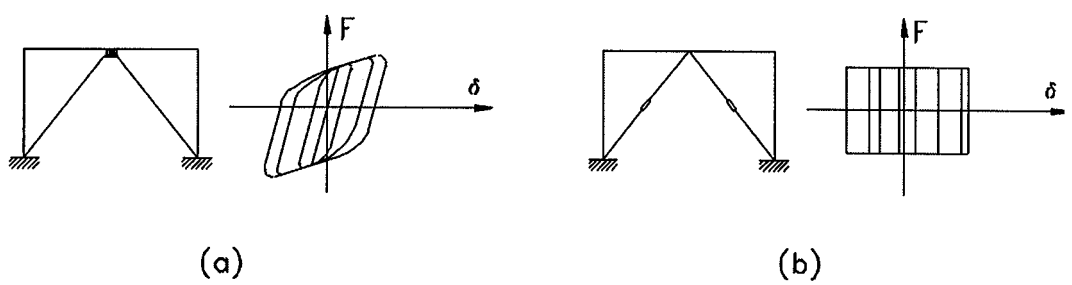

Figure 1. (a) ADAS connection; (b) CFSB connections

where F is the cyclic (axial in CFSB or shear in ADAS) force in the element; d_y is the yielding (ADAS) or sliding (CFSB) displacement; k is the element stiffness $k = F_y/d_y$ (where F_y is the yielding or sliding force); and n is a positive exponential to best represent the hysteretic characteristics of the connection ($n < 1$). The first equation represents the linear elastic branch and the second one simulates the behavior after yielding (or sliding). This model can describe both of the loops depicted in Figure 1. There are three design parameters for each connection: F_y, d_y and n.

In the ADAS devices, based on observations of experimental hysteretic loops and some suggested design guidelines,[15] the selected design parameters are $d_y = 0{\cdot}6$ cm and $n = 0{\cdot}25$. The parameter F_y is selected afterwards. In the CFSB devices, due to its rigid-plastic hysteretic response, $n = 0$ and $d_y = 0$ and therefore the unique design parameter is the sliding threshold force F_y that is also selected next. This force is a function of the friction coefficient and the normal force at the connection. Even though, in general, the friction coefficient varies with the velocity and the actual reactive force during an earthquake, for the purposes of this study a constant coefficient equal to 0·1 is considered.

In this paper, according to Figures 1 and 2, a single ADAS device is installed at each storey and two CFSB connections are placed at each floor (one at every diagonal steel brace). The design criterion consists of selecting their parameters as, for the expected inputs, the maximum interstorey drift is as constant as possible along the height of the building. In this way, the capacity of the main structure is uniformly exploited. This target is achieved in two ways:

(1) The yielding or sliding forces (F_y) in the connections are selected as those generated by the 50, 75 and 100 per cent of the equivalent static lateral loads defined by the UBC-91[16] for normal occupancy building ($I = 1{\cdot}0$), seismic zone 4 ($Z = 0{\cdot}4$), ductile frame ($R_w = 8$) and firm soil ($S = 1{\cdot}0$). This criterion means that, if static and dynamic behaviors were similar, all the devices would simultaneously enter the nonlinear range. Since for a severe earthquake the structure must remain in the linear range and the nonlinearities concentrate in the dissipators, the sliding or yielding forces are equal or less than those induced by strong inputs and the main frame is designed to withstand such loads without yielding.
(2) The forces F_y are constant at each building. This common value is selected as the maximum obtained with the above criterion, which corresponds to the devices located in the lower floor.

Both CFSB devices installed on the same floor are designed for the same sliding force F_y^{CFSB}. Horizontal equilibrium equation shows that this force is proportional to the yielding one F_y^{ADAS} at the ADAS device located at the same level: $F_y^{ADAS} = F_y^{CFSB}\sqrt{2}$ (see Figure 2). Since the displacements in those dissipators are related by the compatibility condition $d_y^{ADAS} = d_y^{CFSB}\sqrt{2}$ it follows that if the hystersis loops were equally shaped they would encompass the same area ($F_y^{ADAS} d_y^{ADAS} = 2F_y^{CFSB} d_y^{CFSB}$) and, consequently, the energy dissipated per cycle would be equal. This permits to compare the performances of both devices.

2.2. *Buildings*

To analyze the response in a wide range of periods, the study includes the buildings with three, seven and fifteen storeys illustrated in Figure 2.

In Figure 2, three 3-bay building structures are represented. The structures are plane frames made of reinforced concrete and incorporate diagonal steel braces; the dissipators are placed at each floor following the schemes shown in Figure 2. The distance between the frames is 6·5 m and it is assumed that each frame carries the load corresponding to that span. The buildings have been designed for gravity and seismic loads. Vertical loads are resisted by the concrete frame and the only purpose of the steel braces is to withstand the horizontal seismic forces. Dead and live loads are each equal to 2500 N/m^2. An equivalent static seismic analysis has been performed assuming that the diagonal members and the main frame are rigidly connected (without dissipators). The UBC equivalent static lateral forces (equal to those considered in the design of the

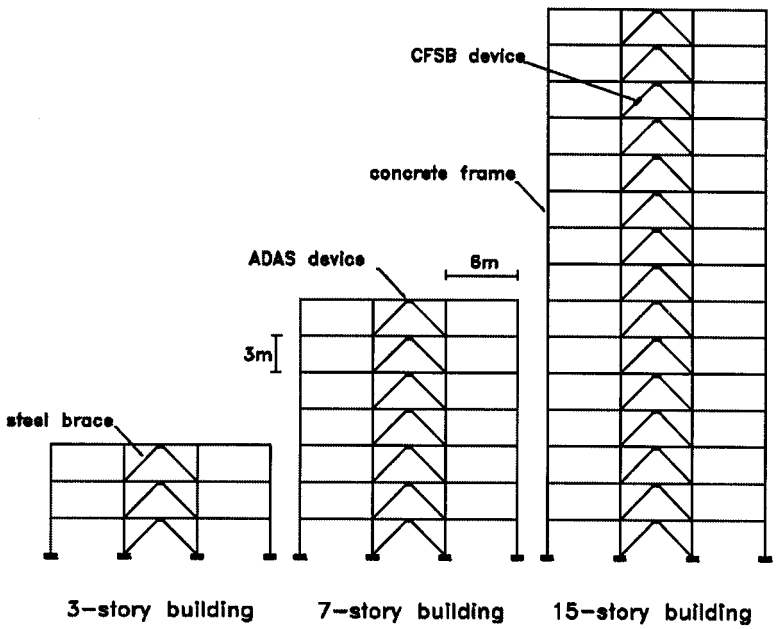

Figure 2. Three basic structural configurations selected for the study

Table I. Main properties of the buildings

No. of floors	Lower columns	Upper columns	T_1 (bare frame) (s)			T_1 (braced frame) (s)		
#	(cm^2)	(cm^2)	(a)	(b)	(c)	(a)	(b)	(c)
3	30·40	30·40	0·74	0·53	0·43	0·28	0·20	0·16
7	30·60	30·40	1·49	1·07	0·87	0·63	0·45	0·36
15	40·60	30·40	3·22	2·32	1·88	1·68	1·21	0·98

dissipators) have been considered. The characteristic value of the concrete compressive strength is $f_{ck} = 25$ MPa and the yielding stress of the reinforcing bars in $f_{yk} = 500$ MPa; the braces are made of FeE235 steel ($f_{yk} = 235$ MPa). The beams and columns have rectangular cross-sections; all the beams are 30 cm wide and 40 cm deep while the cross-sectional dimensions of the columns vary along of the height of the buildings. The steel braces are hollow square tubes, depth and width are equal to 20 cm and the thickness is 5 mm.

In the two columns marked with (b) in Table I the natural periods have been calculated assuming that the mass corresponds to the dead loads and half of the live ones. To consider a wider range of buildings, two additional values of the mass have been considered: the first one is 92 per cent bigger and the second one is 35% smaller; these values have been obtained by modifying the proportion of live loads and the distance between frames. Since the stiffness properties do not change, the periods for these two cases are proportional to those corresponding to the initial value; factors are $\sqrt{1{\cdot}92} = 1{\cdot}39$ (columns marked with (a)) and $\sqrt{0{\cdot}65} = 0{\cdot}81$ (columns marked with (c)), respectively.

In Table I the cross-sectional dimensions of the columns of the three buildings and the fundamental periods T_1 for the three values of mass are described.

Table II. Seismic inputs

Register	Earthquake	Housner intensity (cm)	Peak acceleration (cm s^{-2})	Normalized peak acc. (cm s^{-2})
NS	Lima 1970	28·591	178·951	442·725
	Parkfield 1966	38·898	201·010	374·631
EW	Lima 1970	48·892	192·489	278·495
NOOS	Helena 1935	51·276	143·157	197·485
S21W	Taft 1952	59·167	174·573	208·720
Santa Cruz	Loma Prieta 1989	**70·736**	433·117	433·117
	El Centro 1940	89·848	349·216	274·935
Gilroy	Loma Prieta 1989	113·956	433·616	269·160
Santa Mónica	Northridge 1994	165·426	865·965	370·287
Sylmar	Northridge 1994	388·050	826·760	150·720

In buildings with 7 and 15 storeys, the cross-sectional dimensions of the columns vary gradually from the upper and lower values shown in Table I.

The structure is spatially discretized by a FE code and static condensation is used to obtain a n-DOF 2-D model where n is the number of floors. Mass matrix is diagonal and all the floors have the same mass. Viscous damping matrix is calculated from a modal damping ratio equal to 0·05.

2.3. Seismic inputs

The input consists of ten recorded earthquakes that represent those expected for medium to stiff local soil conditions. The records are normalized with respect to a given Housner intensity. For a particular ground motion the Housner intensity is defined as the area enclosed by the elastic pseudo-spectral velocity spectrum between the periods 0·1 and 2·5 s:

$$H(\zeta) = \int_{0\cdot1}^{2\cdot5} S_v(\zeta, T)\,\mathrm{d}T \tag{2}$$

where ζ is the damping ratio. The reference level of Housner intensity in 71 cm, which corresponds to the Santa Cruz register during the Loma Prieta 1989 earthquake. Table II includes the ground motions along with their Housner intensity (calculated for a damping factor $\zeta = 0{\cdot}05$), peak acceleration and normalized peak acceleration.

Data from Table II show that despite peak accelerations for the Sylmar and Santa Mónica records are very close, their Housner intensity varies by a factor larger than two. This is not surprising since the damage potential of the Sylmar record is larger than the one of the Santa Mónica motion.

3. NUMERICAL ASSESSMENT

In this section the numerical analysis is described and the most representative results are presented. In the first section some plots that illustrate the efficiency of the dissipators are shown and in the second one a sensitivity analysis to the input Housner intensity is performed.

The study mainly consists of calculating the response of the three buildings (with the two variations of mass to alter the natural periods) to the ten normalized inputs. For each building, 14 cases are considered: bare frame (frame without bracing), braced frame (instead of dissipators, there are rigid connections between frame and braces) and frame with ADAS or CFSB (each designed for 50, 75 or 100 per cent of the UBC equivalent loads or their corresponding maximum values). So, this study involves at least $10{\cdot}9{\cdot}14 = 1260$ non-linear analyses.

3.1. Responses to the normalized inputs

Figure 3 presents the average (on the ten inputs) maximum roof displacements (relative to the base) vs. the fundamental period of the braced frame. This figure shows results for the three structural configurations illustrated in Figure 2 and for the aforementioned variations in their natural periods: the three shortest periods correspond to the 3-storey building and the following three and the last three belong, respectively, to the 7- and 15-storey frames (see Table I). The solid thick lines represent the responses for the braced and bare frames assuming linear elastic behavior. Dot and dash lines correspond to similar structures using the CFSB and ADAS devices, respectively. There are three dotted and three dashed lines referring to dissipators designed for 50, 75 and 100 per cent of the UBC-91 equivalent lateral forces, respectively.

Plots from Figure 3 show that the displacements of buildings incorporating. ADAS devices are intermediate between those for bare and braced frames. The displacements of buildings equipped with CFSB are smaller than those with ADAS. For buildings with 7 and 15 storey with CFSB, the maximum displacement can be even lower than the one of the braced frame. This result is remarkable since it is generally accepted that lateral displacements of structures equipped with energy dissipators are larger than those for similar braced ones. This research suggests that this is not the case for medium rise to tall buildings. For both types of dissipators, devices designed for bigger sliding or yielding forces provide smaller displacements.

Figure 4 presents the average of the maximum base shear force (normalized with respect to the total weight of the building) vs. the fundamental period of the braced frame for the cases considered in Figure 3. The figure also includes (thin solid line) the coefficients recommended by the UBC-91 code for a normal occupancy building ($I = 1{\cdot}0$) located in zone 4 ($Z = 0{\cdot}4$) with stiff soil conditions ($S = 1{\cdot}0$) with two global ductility factors: $R_w = 12$ (ductile moment resisting frame) and $R_w = 8$ (a frame with an intermediate level of ductility). In general, the code does not allow to design a building in zone 4 with an intermediate level of ductility but this case is considered here to define a practical design bound for the lateral forces.

Figure 4 shows that the base shear forces using the dissipators (both ADAS and CFSB) are significantly smaller than those for the braced frame and are close to the values for the bare frame. The forces recommended by UBC-91 are smaller but the difference is only important in the small period range.

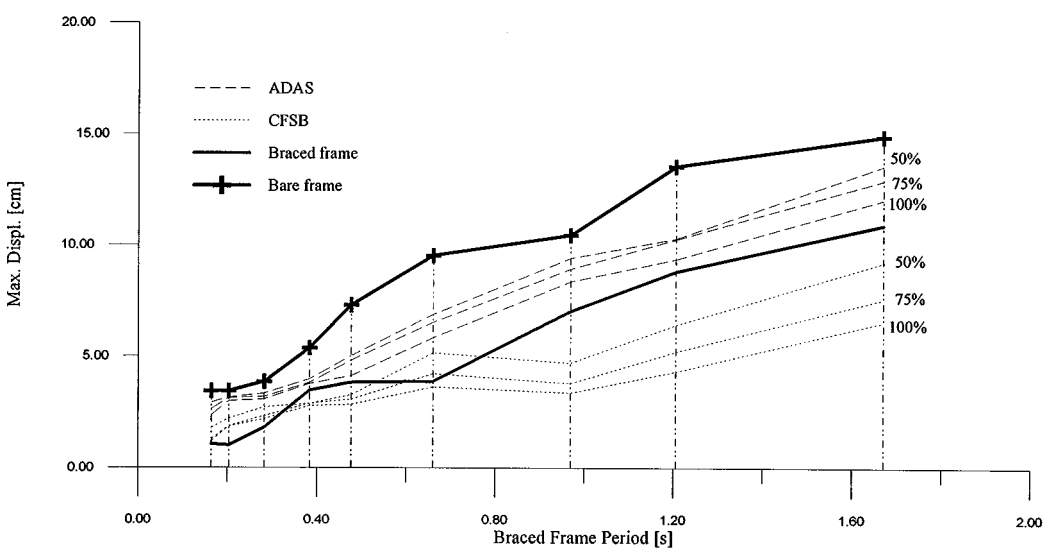

Figure 3. Average maximum top displacements

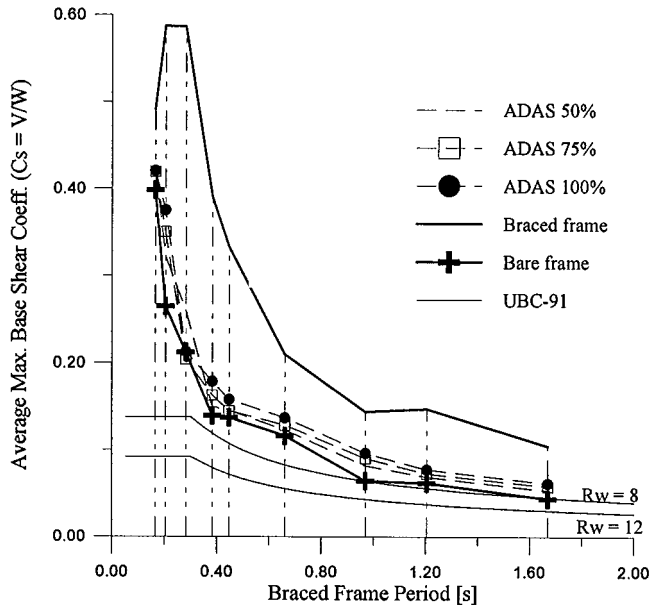

(a)

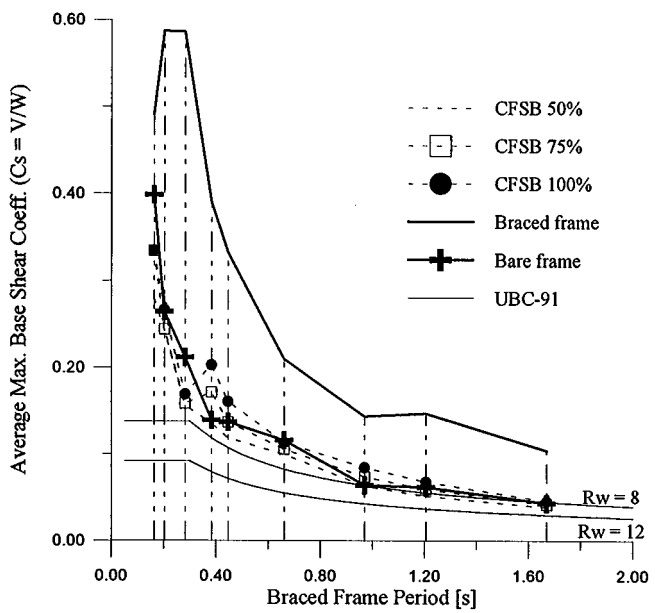

(b)

Figure 4. Average maximum base shear coefficient

Comparisons between left and right plots show that base shear forces are higher for ADAS than for CFSB. Both figures indicate that the bigger the yielding or sliding force the bigger the base shear; however comparison with Figure 3 reveals that augmenting that force pays, since the reduction of the response is important while the increasing of the base shear is less significant.

Table III. Energy dissipated in each ADAS and each pair of CFSB

Floor No.	E_d (kNm) ADAS 75%	E_d (kNm) ADAS 75% (constant)	E_d (kNm) CFSB 75%	E_d (kNm) CFSB 75% (constant)
1	0·028	0·046	3·851	5·921
2	2·306	4·357	10·853	18·946
3	2·584	5·342	9·533	17·798
4	2·347	4·338	8·215	13·710
5	2·343	3·472	7·227	10·309
6	2·537	2·986	6·746	8·031
7	2·103	2·048	6·363	5·633
8	1·616	1·288	6·389	3·765
9	1·811	0·849	6·774	2·491
10	1·206	0·621	7·711	2·072
11	1·466	0·883	8·571	2·420
12	0·921	0·465	6·081	1·517
13	0·218	0·076	2·816	0·418
14	0·029	0·003	1·174	0·043
15	2·02E − 5	5·74E − 5	0·215	0·003
Total	20·795	26·649	92·535	93·085

Figure 4 provides some information about the level of horizontal absolute acceleration in the structure.

Summarizing conclusions from Figures 3 and 4, CFSB devices are more efficient than ADAS ones since they provide higher displacement reduction and transmit less shear force to the ground.

To compare the efficiency of the two proposed design criteria, the average (on the ten inputs) of the energy dissipated in the devices installed at each floor is presented in Table III for the 15 storey building.

In Table III, columns 2 and 4 include the energy dissipated in the ADAS and CFSB when designed according to the equivalent lateral forces from UBC91 (1st criterion in Section 2.1); columns 3 and 5 correspond to F_y constant along the height of the building (2nd criterion in Section 2.1).

Comparison between columns 2 and 3 (and between 4 and 5) show that, if the properties of all the devices are equal, the energy dissipated in the lower floors is bigger than in the case where F_y varies along the height of the building. In the upper floor the situation is opposite and the total energy dissipated is bigger when F_y is constant (the difference for CFSB is less significant than for ADAS). Comparison between columns 2 and 4 (and between 3 and 5) show that the energy dissipated by CFSB is bigger than the one corresponding to ADAS; in the lower and upper floors there is no energy dissipated in the ADAS case. It confirms that CFSB is more efficient than ADAS.

Results in columns 2 and 4 in Table III point out that the energy per unit of sliding force is quite constant in all the floors (except for the lower and upper ones) and consequently the capacity of the dissipators is uniformly exploited. In this sense, the first proposed design criterion is more effective. The performance of ADAS is less uniform along the height.

For buildings with 3 and 7 stories results that are similar to those in Table III are obtained.

To remark the conclusions from Figure 3, the average of the maximum interstorey drift for each floor is plotted in Figure 5 for buildings with 3, 7 and 15 storeys. The value of the mass are those intermediate in Table I (columns b).

Since the yielding displacement d_y for ADAS is equal to 0·6 cm, Figure 5(a) shows that all of these devices in the 3-storey building have entered in the nonlinear range (the maximum ductility demand is equal to 2·25); about the 7- and 15-storey frames, Figures 5(b) and 5(c) show that some ADAS dissipators might not reach the yielding point (in an average sense).

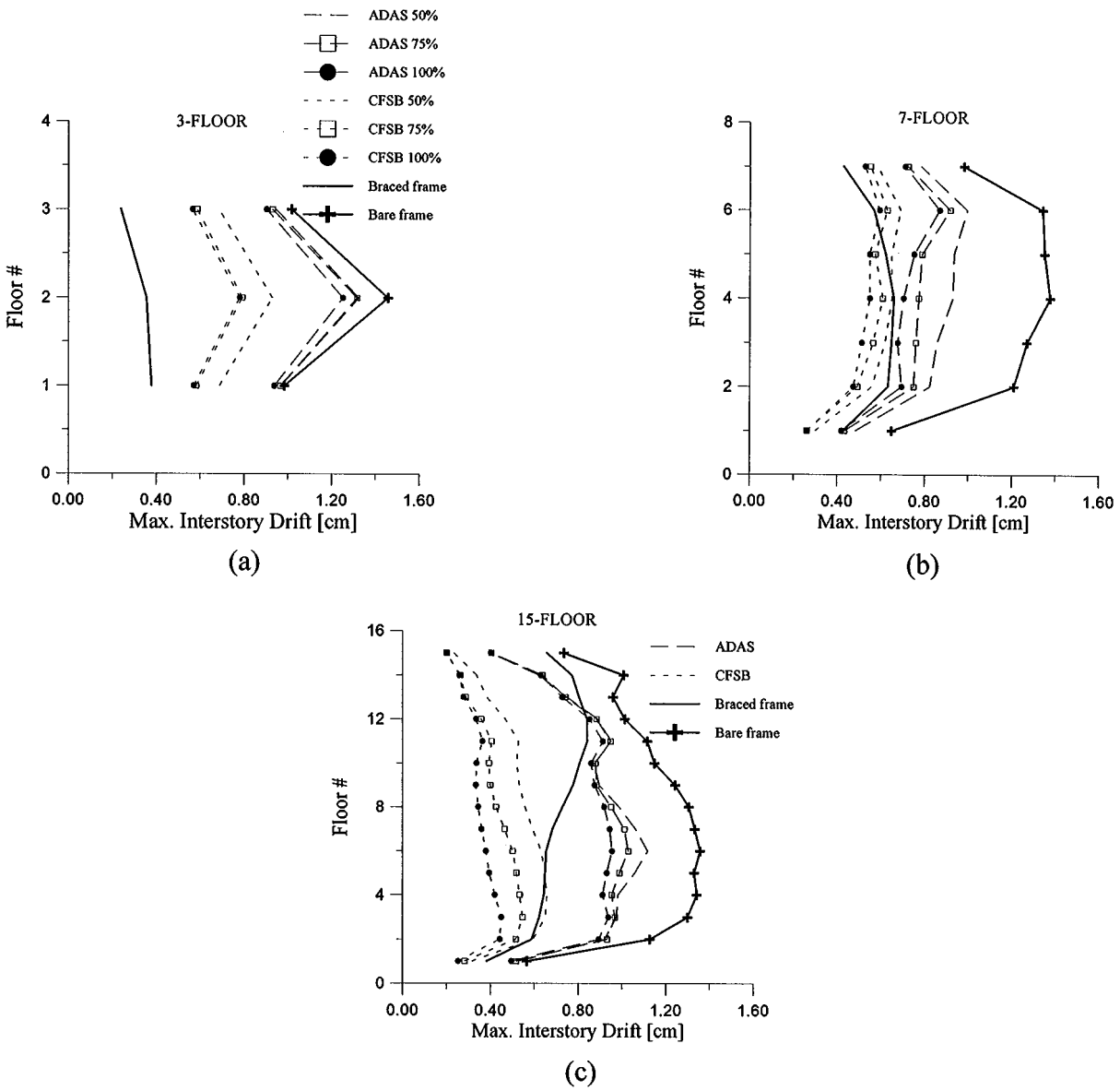

Figure 5. Average maximum interstorey drift

To assess the influence of the variation of the cross-sectional properties of the columns along the height, another 15-storey building with uniform columns has been considered. The cross-sectional dimensions of the columns are 40 and 60 cm. The fundamental period of the braced frame is 1·19 s and the one of the bare frame is 2·29 s. The mass is equal to the intermediate one in Table I (columns b). The dissipators have designed as in Figure 5.

Comparison between Figures 6 and 5(c) shows that the behavior of both buildings is similar. The only significant difference is that, as expected, the interstorey drifts in the upper floors are smaller for the building with uniform columns (Figure 6). As well, the average values of the ratio maximum base shear/total weight are close to those shown in Figure 4.

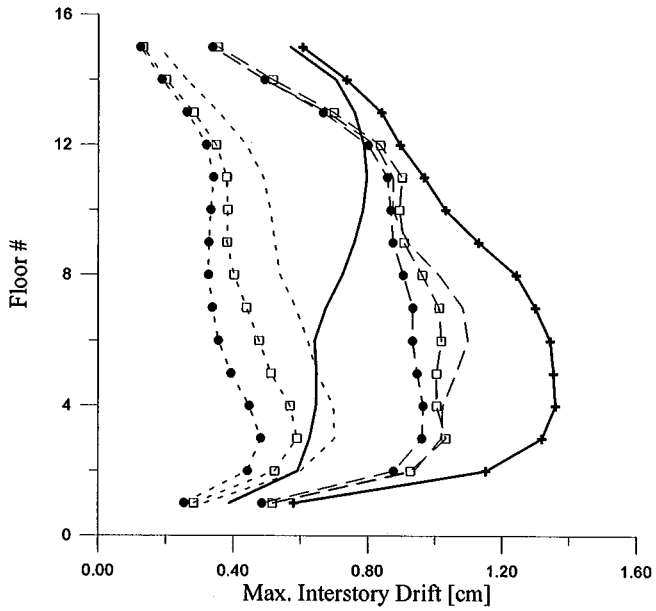

Figure 6. Average maximum interstorey drift for 15-storey frame with uniform columns

As an index of the performance of the dissipators, the ratio energy dissipated in the devices/input energy, has been calculated for the building considered in Figure 6 for Sylmar register (see Table II) For the ADAS device the values are 0·272 (50 per cent), 0·298 (75 per cent) and 0·336 (100 per cent); for the CFSB are 0·803 (50 per cent), 0·840 (75 per cent) and 0·857 (100 per cent). These results show again that rigid-plastic devices are more efficient to dissipate energy.

To evaluate the influence of the variation of F_y along the height of the building, the average values (on the ten inputs) of the maximum interstorey drifts for buildings with 3, 7 and 15 storeys are plotted in Figure 7 for the two design criteria described in Section 2.1. The mass is the same as in Figure 5.

Plots from Figure 7 show that, using the same dissipators in the whole building (2nd design criterion in Section 2.1), the interstorey drift is bigger in the lower floors and smaller in the upper ones. It means that, if F_y is constant in the building, the structure is stiffer and 'soft-storey' behaviour[17] is more relevant. As well, CFSB is more efficient than ADAS.

To assess the robustness of the system, the consequences of failure of some dissipators have been investigated. As an example, in Table IV the maximum interstorey drifts for Sylmar earthquake (it has been selected because it possesses the biggest Housner intensity as shown in Table II) are presented for the seven storey building (mass corresponds to columns a in Table I) equipped with ADAS devices designed for the 75 per cent of the forces generated by the equivalent lateral loads from UBC-91. The failure consists of given percentages of reduction (50 and 90 per cent) in the yielding forces F_y for the dissipators located in 1st and 5th levels. It could correspond to partial failures in ADAS or CFSB devices.

Results from Table IV show that the system is robust since the only effect of the reduction in the sliding force is a slight increase (about 11 per cent if F_y is reduced by 50 per cent and 20 per cent if the percentage of reduction reaches 90%) in the interstorey drift in the floor where the failures occur. Less growth has generated in the adjacent floors. Values in italics are smaller than d_y (0·6 cm) and therefore correspond to no energy dissipated.

Similar conclusions are derived for other close situations and for buildings with 3 and 15 storeys.

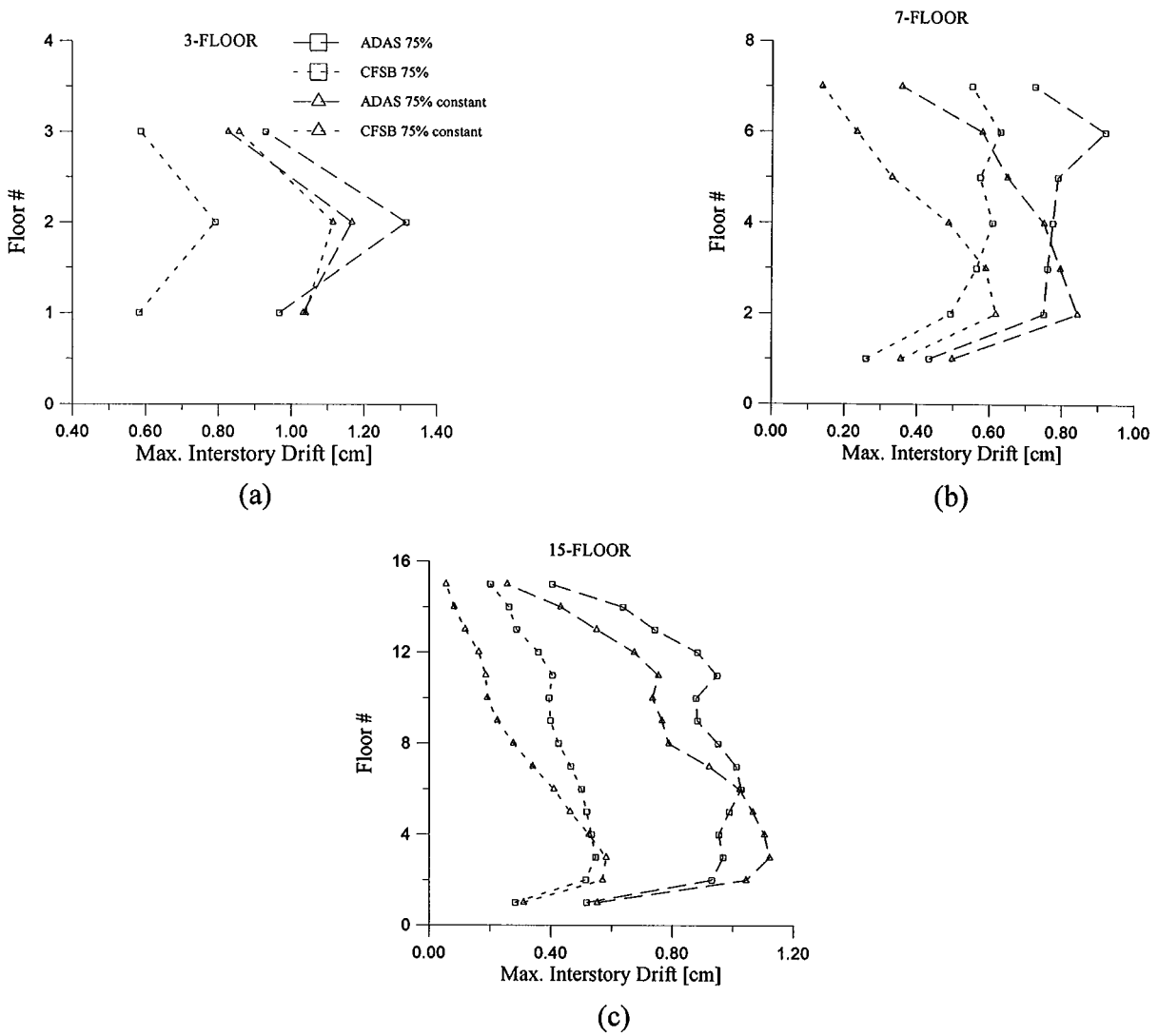

Figure 7. Average maximum interstorey drift for two different design criteria of ADAS and CFSB

Table IV. Maximum interstorey drifts (cm) when some dissipators partially fail. Sylmar earthquake. ADAS 75 per cent

Floor no.	No. failure F_y 0% reduction	1st floor F_y 50% reduction	5th floor F_y 50% reduction	1st and 5th floor F_y 50% reduction	1st floor F_y 90% reduction	5th floor F_y 90% reduction	1st and 5th floor F_y 90% reduction
1	*0·324*	***0·359***	*0·308*	***0·339***	***0·391***	*0·296*	***0·370***
2	*0·595*	0·620	*0·550*	*0·572*	0·641	*0·506*	*0·541*
3	0·675	0·674	0·647	0·644	0·670	0·619	0·606
4	0·784	0·778	0·828	0·820	0·768	0·858	0·833
5	0·815	0·813	**0·907**	**0.904**	0·808	**0·979**	**0·974**
6	0·814	0·818	0·899	0·904	0·820	0·974	0·987
7	*0·511*	*0·506*	*0·507*	*0·506*	*0·502*	*0·526*	*0·522*

3.2. Responses to the scaled inputs

In this subsection a sensitivity analysis to the Housner intensity of the earthquakes is performed. To do this, the ten seismic inputs described in Table II are scaled by factors 1/2·5, 1 and 2·5, so providing Housner intensities equal to 28, 71 and 177, respectively. In Figure 8 the average values (for the ten scaled inputs) of the

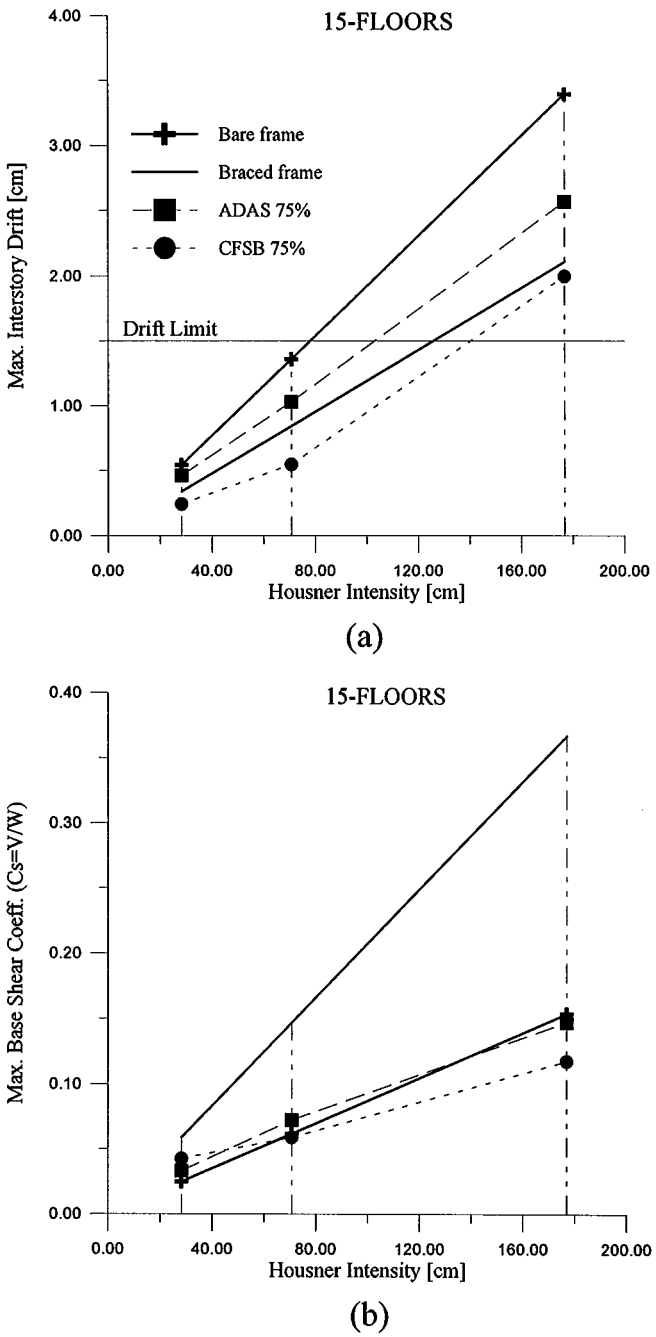

Figure 8. Average maximum interstorey drift (a) and base shear coefficient (b) for different Housner intensities

maximum interstorey drift and the maximum base shear coefficient are plotted vs. the Housner intensity for the building with 15 storeys. Four cases have been considered: bare and braced frames, ADAS 75 per cent and CFSB 75 per cent. The values of the mass are those intermediate (columns a in Table I). In Figure 7a the horizontal thin solid line represents the drift limitation by the UBC-91 code.

The bare and braced frames are assumed to behave linearly and, consequently, the corresponding curves in Figures 8(a) and 8(b) are also linear. In Figure 8(a) the curve for ADAS is roughly linear while the one for CFSB is clearly non-linear, using the dissipator the maximum interstorey drift for Housner intensity equal to 177 is bigger than the one if the behaviour would be linear, it shows that the performance of the device decreases as the input intensity increases. In Figure 8(b) the curves for ADAS and CFSB are slightly nonlinear; as the input intensity augments, the base shear coefficient decreases for ADAS and increases for CFSB.

Similar conclusions can be derived for 3- and 7-storey buildings.

4. CONCLUSIONS AND FUTURE RESEARCH

The main conclusions of this paper are:

(1) ADAS and CFSB are useful to reduce the maximum interstorey drift compared to the bare frame. The maximum base shear forces are similar regardless of the type of dissipator and their yielding or sliding forces. The aforementioned values are close to those for the bare frame.
(2) For the particular design criteria considered in this paper, CFSB is more efficient than ADAS since its maximum interstorey drift is smaller and is quite uniform along the height of the buildings. For the 7- and 15-storey frames, it can be even less than the braced frame. The difference between the performances of both types of dissipators can be explained because in the friction device (CFSB) the area included in the hysteresis loop is bigger and, due to its rigid-plastic behaviour, it starts dissipating energy (smaller interstorey drift) before the yielding device (ADAS) does.
(3) The proposed design criteria provide good results since the maximum interstorey drift and the ratio energy dissipated/design force are quite constant along the height of the building. Most of the input energy is dissipated in the ADAS and CFSB devices.
(4) The system is robust with respect to local failures in some dissipators.

These observations motivate the search towards a rigid-plastic device (such as the CFSB one) based on the plastification of metals instead of friction. An experimental study is being performed at the University of Girona with a shear dissipator.

ACKNOWLEDGMENTS

This work has received financial support from Spanish Government (DGICYT), Research Project No. PB92-075. The stay of D. Foti at Barcelona has been supported by the European Commission, Human Capital and Mobility Grant No. ERBCHBICT941821.

REFERENCES

1. I. D. Aiken and J. M. Kelly, 'Earthquake simulator testing and analytical studies of two energy-absorbing systems for multistorey structures', *UCB/EERC Report No UCB/EERC 90/03*. Earthquake Engineering Research Center, Berkeley, 1990.
2. J. A. Inaudi and J. M. Kelly, 'A friction mass damper for vibration control', *Report No UCB/EERC 92/15*, Earthquake Engineering Research Center, Berkeley, 1992.
3. C. Xia and R. D. Hanson, 'Influence of ADAS element parameters on building seismic response', *J. Struct. Engng. ASCE* **118**, 1903–1918 (1992).
4. M. Nakashima and K. Saburi, 'Energy input and dissipation behaviour of structures with hysteretic dampers', *Earthquake Engng. Struct. Dyn.* **25**, 483–496 (1996).
5. S. E. Ruiz, O. E. Urrego and F. L. Silva, 'Influence of the spatial distribution of energy-dissipating bracing elements on the seismic response of multistorey frames', *Earthquake Engng. Struct. Dyn.* **24**, 1511–1525 (1995).

6. A. Filiatrault and S. Cherry, 'A Simplified Design Procedure for Friction Damped Structures', *Proc. 4th U.S. Nat. Conf. on Earthquake Engineering*, Vol. 3, pp. 479–488, Palm Springs, 1990.
7. P. Colajanni and M. Papia, 'Energy design approach for braced frames with dissipative devices', *Proc. 11WCEE*, Paper No. 354, Acapulco, Mexico, 1996.
8. R. Levy, J. Gluck and N. Gluck, 'Optimal design of supplemental dampers for control structures', *Proc. 11WCEE*, Paper No. 1538, Acapulco, Mexico (1996).
9. Y.-F. Su and R. D. Hanson, 'Comparison of effective supplemental damping equivalent viscous and hysteretic', *Proc. 4th U.S. Nat. Conf. Earthquake Engineering*, pp. 507–516, Palm Springs, 1990.
10. W. S. Pong, C. S. Tsai and G. C. Lee, 'Seismic Study of Building Frames with Added Energy-Absorbing Devices', *Technical Report No NCEER-94-0016*, State University of New York, Buffalo, 1994.
11. E. L. Wilson, 'SADSAP, Static and Dynamic Structural Analysis Programs', *Structural Analysis Programs Inc*., 1992.
12. D. Foti, '*Numerical and Experimental Efficiency Assessment of Energy Dissipators of Seismic Protection of Buildings*', Technical University of Catalonia, Catalonia, 1998.
13. R. Scholl, 'Improve the Earthquake Performance of Structures with Added Damping and Stiffness Elements', *Proc. 4th U.S. Nat. Conf. Earthquake Engineering*, Vol. 3, pp. 489–498, Palm Springs, 1990.
14. Z. Akbay and H. M. Aktan, 'Intelligent Energy Dissipation Devices', *Proc. 4th U.S. Nat. Conf. Earthquake Engineering*, 427–435, Palm Springs, 1990.
15. R. D. Hanson, C. Xia and Y. F. Su, 'Design of Supplemental Steel Damping Devices for Buildings', *Proc. 10WCEE*, 4139–4142. Madrid, Spain (1992).
16. Uniform Building Code, *Int. Conf. of Build. Off*., Whittier, California, 1991.
17. L. Bozo and A. Barbat, 'Técnicas avanzadas de diseño sismorresistente', CAPECO, Perú, 1994.

